Computational and Applied Mathematics (2022) 41: 320
https://doi.org/10.1007/s40314-022-02028-5

Optimal mitigation of atmospheric carbon dioxide through forest management programs: a modeling study

Maitri Verma[1] · **Cherie Gautam**[1]

Received: 30 March 2022 / Revised: 14 August 2022 / Accepted: 4 September 2022 /
Published online: 21 September 2022

Abstract
The rising level of atmospheric carbon dioxide (CO_2) gas is a matter of concern due to its impact on global climate change. The accomplishment of the goal of climate change mitigation requires a reduction in the CO_2 concentration in near future. The forest management programs offer an avenue to regulate atmospheric CO_2 levels. This paper presents a four-dimensional nonlinear mathematical model to study the impact of forest management policies on the mitigation of atmospheric CO_2 concentrations. It is assumed that forest management programs are applied according to the difference of forest biomass density from its carrying capacity. The forest management programs are assumed to work twofold: first, they increase the forest biomass and secondly they reduce the deforestation rate. Model analysis shows that the atmospheric level of CO_2 can be effectively curtailed by increasing the implementation rate of forest management options and their efficacy. It is found that as the deforestation rate coefficient exceeds a critical value, loss of stability of the interior equilibrium state occurs and sustained oscillations arise about interior equilibrium through Hopf-bifurcation. The stability and direction of bifurcating periodic solutions are discussed using center manifold theory. Further, it is observed that the amplitude of periodic oscillation dampens as the maximum efficacy of forest management programs to reduce the deforestation rate increases and above a critical value of the maximum efficacy of forest management programs, the periodic oscillations die out and the interior equilibrium becomes stable. The strategies for the optimal control of CO_2 concentration while minimizing the execution cost of forest management programs are also investigated using the optimal control theory. The theoretical results are demonstrated via numerical simulations.

Keywords Mathematical model · Global warming · Forest management · Stability · Hopf-bifurcation · Optimal control

Mathematics Subject Classification 34D05 · 34D20 · 34D23 · 92B05

Communicated by Valeria Neves Domingos Cavalcanti.

✉ Maitri Verma
maitri.verma9@gmail.com

[1] Department of Mathematics, School of Physical and Decision Sciences, Babasaheb Bhimrao Ambedkar University, Lucknow 226025, India

1 Introduction

The past few decades witnessed a rapid rise in atmospheric carbon dioxide (CO_2) concentrations. The excessive increase in carbon dioxide levels has negative impacts on air quality and human health, and is the prime driver of the problem of global warming. Global warming has many adverse effects on the humans and ecosystem, like melting of ice covers and permafrost, storm surges, flood and erosion in the coastal regions, increase in the chances of extinction of endangered animal and plant species, change in rainfall patterns affecting global food and water supply, increase in vector-borne, food-borne and water-borne diseases, increase in heat-related illness, etc. (McMichael et al. 2006; Casper 2010; Shuman 2010; Yang et al. 2021). The carbon dioxide concentration has reached a level of 418 ppm in the year 2022, which is approximately 49% above the level of 280 ppm that existed at the beginning of the industrial revolution (Prentice et al. 2001; NOAA 2022). Deforestation is one of the largest human-caused sources of CO_2 emissions. Since 1990, nearly 420 million ha (hectare) of forests are lost worldwide due to deforestation with an annual rate of 10 million ha per year between 2015-2020 (FAO 2020). Reforestation and afforestation activities are of great importance to compensate for the forest loss caused by deforestation and are adopted by many countries across the globe. The reforestation rate in 2015 was estimated to be 27 million ha with an annual increase of 1.57 % (FAO 2016). To attain the objective of mitigation of increased carbon dioxide levels in the atmosphere, plantation on a large scale is required, however, a number of demographic and economic constraints restrict reforestation on the desired scale (Jackson and Baker 2010). In this scenario, countries are adopting forest management policies that increase forest biomass and reduce deforestation rates, thus aiding in reducing the atmospheric burden of CO_2. Costa Rica is the first tropical country that has successfully reversed the deforestation and restored forest cover from 24.4% in 1985 to more than 50% by 2011 using the forest management policies (Tafoya et al. 2020).

Worldwide concern about the degradation of forests is leading to new approaches to forest management. Use of the genetically engineered plants having elongated roots, high growth rate, and biomass productivity is one of the emerging techniques to increase the forest biomass per unit forest area and reduce the atmospheric level of carbon dioxide (Harfouche et al. 2011; Ye et al. 2011; Dubouzet et al. 2013; Chang et al. 2018; Verma et al. 2021). In Brazil, the genetically modified eucalyptus trees are found to grow faster and absorb more carbon dioxide, resulting in larger forest biomass productivity per unit area (Ledford 2014). Agroforestry is another practice widely used nowadays to increase productivity and forest cover. Agroforestry refers to a land-use system that integrates trees in farms and agriculture landscapes to enhance productivity and ecosystem sustainability (Zomer et al. 2016). In many countries, agroforestry is considered to be an important part of the overall regional strategy for forest management and climate change mitigation (Van Noordwijk et al. 2003). The average carbon sequestration potential of Indian agroforestry is estimated to be 25 tonnes of carbon per hectare (Basu 2014). The rural population relies very much on the forests for their livelihood, fuel for cooking and heating purposes, etc. The dependence of the population on forestry resources is often a result of a lack of availability of alternatives to the forest resources or the inability of the population to afford them (Badola et al. 2012). The programs that provide economic incentives to the rural people for their livelihood, like fuel efficient stoves and biogas, fiber, tin, subsidy on those products which are the alternate of forest resources, etc., are fruitful to reduce the deforestation rates (Misra and Lata 2015a). In recent years, many climate change mitigation frameworks are developed that focus on the reduction of carbon dioxide emissions from deforestation and forest degradation. One

of the main international policies in this regard is developed by UNFCCC (United Nations Framework Convention on Climate Change) Conference of the Parties, which is known as REDD+ (reducing emissions from deforestation and degradation plus) mechanism. REDD+ mechanism is aimed to guide and provide economic support to the activities in the forest sector which reduces the deforestation rate and increases the existing forest carbon stocks using sustainable forest management (UNFCCC 2010; Bottazzi et al. 2013). It is found that a national-level REDD+ program can significantly reduce the forest cover loss and associated carbon emissions. A study has shown that the Norway-Guyana REDD+ program caused a decrease in the tree cover loss by 35% during the period 2010 to 2015 and avoided 12.8 million tons of CO_2 emissions (Roopsind et al. 2019). Thus, the forest management activities contribute significantly in reduction of deforestation rate and enhancement of forest biomass.

In recent years, several mathematical models are proposed to explore the effect of various factors, including human population and forest biomass, on the dynamics of CO_2 gas in the atmosphere (Tennakone 1990; Lonngren and Bai 2008; Caetano et al. 2011; Misra and Verma 2013, 2015; Misra et al. 2015; Shukla et al. 2015; Verma and Misra 2018; Devi and Gupta 2018, 2020; Devi and Mishra 2020; Verma et al. 2021; Verma and Verma 2021; Misra and Jha 2021). In particular, Tennakone (1990) has proposed a simple mathematical model to examine the stability conditions of the biomass and atmospheric CO_2 equilibrium. It is found that for a critically high deforestation rate, the biomass-carbon dioxide equilibrium may become unstable accompanied by an increase in CO_2 concentration. Misra and Verma (2013) have proposed a three-dimensional model to assess the interplay between the human population, forest biomass and atmospheric CO_2. In this study, it is found that the deforestation rate has destabilizing effect over system's dynamics. Further, Misra et al. (2015) have proposed a mathematical model to examine the effect of delay involved in applying reforestation efforts on the control of CO_2 levels in the atmosphere. Devi et al. (2018) presented a study of the effect of the varying capability of plants to uptake CO_2 on atmospheric CO_2 levels. Misra and Jha (2021) have developed a mathematical framework to study the effect of population pressure on the dynamics of carbon dioxide gas. They have found that an increase in the reduction rate coefficient of forest biomass due to population pressure leads to an increase in the equilibrium CO_2 level. Many studies presented nonlinear mathematical models for the conservation of forest biomass (Shukla and Dubey 1997; Dubey et al. 2009; Misra and Lata 2015a, b; Lata and Misra 2017). These studies show that the forest biomass can be conserved using technological efforts like plantation of genetically engineered plants and providing economic incentives to the people which ultimately reduce the deforestation rate. However, these studies do not explore the effect of forest conservation on the CO_2 levels. In the present study, we have formulated a mathematical model to study the impact of forest management programs on atmospheric CO_2 levels. We have assumed that the forest management programs focus to reduce the deforestation rate via providing economic incentives and motivating people to switch to alternate resources. Apart from reducing the deforestation rates, these programs also focus to increase the forest biomass through afforestation, plantation of genetically modified trees, etc.

2 The model

Consider a geographical region in which forests are depleting due to an increase in the human population. The forest management programs are executed to reduce the deforestation rate and increase the forest biomass. Forest biomass is one of the prime sinks of carbon dioxide,

so the depletion and conservation of forest biomass will affect the dynamics of atmospheric carbon dioxide. To model this scenario, we have considered four dynamic variables, namely the atmospheric CO_2 concentration ($C(t)$), human population ($N(t)$), forest biomass ($B(t)$), and a measure of forest management programs ($P(t)$). The forest management programs can be measured in terms of their execution cost. The natural emission rate of carbon dioxide is assumed to be a constant while the anthropogenic emission rate is considered to be proportional to the human population (Onozaki 2009; Jorgenson and Clark 2013). The removal rate of CO_2 by forest biomass during photosynthesis is assumed to depend on both the concentration of carbon dioxide and the density of forest biomass. It is also assumed that the CO_2 removal rate by other natural sinks, like ocean, etc., is proportional to atmospheric CO_2 concentration (Nikol'kii 2010). Under the above assumptions, the dynamics of CO_2 is given as

$$\dot{C} = Q + \lambda N - \alpha C - \lambda_1 BC. \tag{1}$$

In the above equation $\dot{C}$ denotes time derivative of $C(t)$, Q is the natural emission rate of CO_2, λ is the anthropogenic emission rate coefficient of CO_2, λ_1 and α are the uptake rate coefficients of CO_2 from the atmosphere by forest biomass and natural sinks other than forest biomass, respectively.

The population and forest biomass are assumed to grow logistically. The population cut down forests for their use which supports the population growth. Thus, an increase in population is assumed to reduce forest biomass while an increase in biomass boosts population growth. Further, it is considered that the implementation of forest management programs causes a reduction in deforestation rate and an increase in forest biomass. The reduction in deforestation rate due to forest management programs can not increase indefinitely with the increase in management programs so it is taken as a saturating function of forest management programs. Similarly, the forest biomass can not be increased indefinitely with an increase in management programs, therefore we have taken that growth rate of forest biomass due to the application of management programs as a saturating function of management programs. The Earth's surface temperature will increase due to the increase in radiative forcing created by enhanced atmospheric CO_2 concentration (IPCC 2014). The climate changes caused by enhanced surface temperature have many adverse impacts on the population (Ichikawa 2004; McMichael et al. 2006; Kurane 2010; Misra 2014); therefore, it is considered that population declines due to elevated CO_2 concentration. Under these assumptions, the following differential equations capture the dynamics of population and forest biomass:

$$\dot{N} = sN\left(1 - \frac{N}{L}\right) + \xi NB - \theta CN, \tag{2}$$

$$\dot{B} = uB\left(1 - \frac{B}{M}\right) - \left(\phi - \frac{\phi_1 P}{k_1 + P}\right)NB + \frac{\eta_1 PB}{l_1 + P}. \tag{3}$$

In the above differential equations, s and L are the intrinsic growth rate and carrying capacity of the population, respectively. The constant ξ is the growth rate coefficient of the population due to forest biomass and θ is the declination rate coefficient of population due to an increase in CO_2 level. The constants u and M are the intrinsic growth rate and carrying capacity of forest biomass, respectively. ϕ is the deforestation rate coefficient whereas ϕ_1 and η_1 denote the maximum efficiencies of forest management programs to reduce the deforestation rate and to increase the forest biomass, respectively. The constant k_1 is a half-saturation constant representing the level of forest management programs at which half of the maximum reduction in deforestation rate due to forest management programs is reached. The constant l_1 is a half-

saturation constant representing the level of forest management programs at which half of the maximum increase in growth rate of forest biomass due to forest management programs is reached.

We assumed that forest management programs are implemented at a rate proportional to the difference of current forest biomass density from its carrying capacity. Some of the forest management programs will diminish due to their ineffectiveness or some economical barriers. Let ν and ν_0 denote the implementation and declination rate coefficients of forest management programs, respectively, then the dynamics of forest management programs is given as

$$\dot{P} = \nu(M - B) - \nu_0 P. \tag{4}$$

Thus, the following model describes the dynamics of the problem:

$$\begin{aligned}
\dot{C} &= Q + \lambda N - \alpha C - \lambda_1 BC,\\
\dot{N} &= sN\left(1 - \frac{N}{L}\right) + \xi NB - \theta CN,\\
\dot{B} &= uB\left(1 - \frac{B}{M}\right) - \left(\phi - \frac{\phi_1 P}{k_1 + P}\right)NB + \frac{\eta_1 PB}{l_1 + P},\\
\dot{P} &= \nu(M - B) - \nu_0 P,
\end{aligned} \tag{5}$$

where $C(0) = C_0 > 0, N(0) = N_0 \geq 0, B(0) = B_0 \geq 0$ and $P(0) = P_0 \geq 0$. All the parameters of system (5) are positive constants.

2.1 Region of attraction

The region of attraction for all solution of system (5) initiating in positive orthant is given by set

$$\Gamma = \{(C, N, B, P) : 0 < C \leq C_m; 0 \leq N \leq N_m; 0 \leq B \leq M; 0 \leq P \leq P_m\},$$

where $C_m = (Q + \lambda N_m)/\alpha$, $N_m = L + (\xi LM/s)$ and $P_m = \nu M/\nu_0$.

3 Mathematical analysis of system(5)

To analyze the qualitative behavior of the dynamical system (5), we employ the stability theory of differential equations. We find the equilibrium points and check the stability behavior of these equilibrium points to access the behavior of the system in the long term.

3.1 Equilibrium analysis

System (5) has four nonnegative equilibria, which are listed below:

1. $S_1\left(\frac{Q}{\alpha}, 0, 0, \frac{\nu M}{\nu_0}\right)$ always exists.
2. $S_2\left(\frac{Q}{\alpha+\lambda_1 M}, 0, M, 0\right)$ always exists.
3. $S_3(C_3, N_3, 0, P_3)$ exists, provided the following condition is satisfied:

$$s - \frac{\theta Q}{\alpha} > 0, \tag{6}$$

where $C_3 = \frac{s(Q+\lambda L)}{s\alpha+\theta\lambda L}$, $N_3 = \frac{L(s\alpha-\theta Q)}{s\alpha+\theta\lambda L}$, $P_3 = \frac{\nu M}{\nu_0}$.

4. $S^*(C^*, N^*, B^*, P^*)$ exists, provided the following conditions are satisfied :

$$u - \left(\phi - \frac{\phi_1 \nu M}{k_1\nu_0 + \nu M}\right)\left(\frac{s\alpha - \theta Q}{s\alpha + \theta\lambda L}\right)L + \frac{\eta_1 \nu M}{l_1\nu_0 + \nu M} > 0, \tag{7}$$

$$s - \frac{\theta Q}{\alpha + \lambda_1 M} + \xi M > 0. \tag{8}$$

The existence of equilibria S_1, S_2 and S_3 is obvious. In the following, the existence of equilibria S^* is established. The values of components C^*, N^*, B^* and P^* may be obtained by solving the following set of algebraic equations:

$$Q + \lambda N - \alpha C - \lambda_1 BC = 0, \tag{9}$$

$$s\left(1 - \frac{N}{L}\right) + \xi B - \theta C = 0, \tag{10}$$

$$u\left(1 - \frac{B}{M}\right) - \left(\phi - \frac{\phi_1 P}{k_1 + P}\right)N + \frac{\eta_1 P}{l_1 + P} = 0, \tag{11}$$

$$\nu(M - B) - \nu_0 P = 0. \tag{12}$$

From equation (12), we have

$$P = \frac{\nu(M - B)}{\nu_0} = q(B). \tag{13}$$

From equation (9), we have

$$C = \frac{Q + \lambda N}{\alpha + \lambda_1 B}. \tag{14}$$

Using equation (14) in equation (10) , we have

$$N = L\left[\frac{(s + \xi B)(\alpha + \lambda_1 B) - \theta Q}{s(\alpha + \lambda_1 B) + \theta\lambda L}\right] = g(B). \tag{15}$$

Using equation (13) and equation (15) in equation (11), we obtain the following equation in B:

$$h(B) = u\left(1 - \frac{B}{M}\right) - \left(\phi - \frac{\phi_1 q(B)}{k_1 + q(B)}\right)g(B) + \frac{\eta_1 q(B)}{l_1 + q(B)} = 0. \tag{16}$$

From equation (16), we may easily note that

(i)

$$h(0) = u - L\left(\phi - \frac{\phi_1 \nu M}{k_1\nu_0 + \nu M}\right)\left(\frac{s\alpha - \theta Q}{s\alpha + \theta\lambda L}\right) + \frac{\eta_1 \nu M}{l_1\nu_0 + \nu M},$$

which is positive under the condition (7).

(ii)

$$h(M) = -\phi g(M) = -\phi L\left[\frac{(s + \xi M)(\alpha + \lambda_1 M) - \theta Q}{s(\alpha + \lambda_1 M) + \theta\lambda L}\right],$$

which is negative under the condition (8).

(iii) The derivative of $h(B)$ w.r.t. B is given by

$$h'(B) = -\frac{u}{M} - \left(\phi - \frac{\phi_1 q(B)}{k_1 + q(B)}\right) g'(B) + g(B)\frac{k_1\phi_1 q'(B)}{(k_1 + q(B))^2} + \frac{l_1\eta_1 q'(B)}{(l_1 + q(B))^2}$$
$$< 0 \text{ for } B \in (0, M),$$

as

$$g'(B) = L\left[\frac{s\xi(\alpha + \lambda_1 B)^2 + s\lambda_1\theta Q + \theta\lambda L\xi(\alpha + \lambda_1 B) + \theta\lambda L\lambda_1(s + \xi B)}{(s(\alpha + \lambda_1 B) + \theta\lambda L)^2}\right] > 0,$$

and $q'(B) = -\frac{\nu}{\nu_0} < 0$.

Thus, a unique positive root B^* of equation (16) lies in the interval $(0, M)$ provided the conditions (7) and (8) hold. Using this value of B^* in equations (13)-(15), we get the positive values of $P = P^*$, $C = C^*$ and $N = N^*$, respectively.

3.2 Local stability analysis

The behavior of the trajectories starting in a small neighbourhood of non-negative equilibria S_1, S_2, S_3 and S^* of system (5) are examined and the following results are obtained:

Theorem 1 (i) *The equilibrium S_1 is always unstable.*
(ii) *The equilibrium S_2 is unstable whenever S^* exists.*
(iii) *The equilibrium S_3 is unstable whenever S^* exists.*
(iv) *The equilibrium S^* is locally asymptotically stable iff the following condition holds*

$$D_3(D_1D_2 - D_3) - D_1^2 D_4 > 0, \tag{17}$$

where $D_i (i = 1, 2, 3, 4)$ are defined in the proof.

Proof The Jacobian matrix $\hat{J}$ for system (5) is given by:

$$\hat{J} = \begin{pmatrix} -(\alpha + \lambda_1 B) & \lambda & -\lambda_1 C & 0 \\ -\theta N & s\left(1 - \frac{2N}{L}\right) + \xi B - \theta C & \xi N & 0 \\ 0 & -\left(\phi - \frac{\phi_1 P}{k_1 + P}\right) B & u\left(1 - \frac{2B}{M}\right) - \left(\phi - \frac{\phi_1 P}{k_1 + P}\right) N + \frac{\eta_1 P}{l_1 + P} & \frac{\phi_1 k_1 N B}{(k_1 + P)^2} + \frac{\eta_1 l_1 B}{(l_1 + P)^2} \\ 0 & 0 & -\nu & -\nu_0 \end{pmatrix}.$$

Let $\hat{J}_{S_1}$, $\hat{J}_{S_2}$, $\hat{J}_{S_3}$ and $\hat{J}_{S^*}$ are the Jacobian matrix $\hat{J}$ evaluated at S_1, S_2, S_3 and S^*, respectively. Then (i) The eigenvalues of $\hat{J}_{S_1}$ are $-\alpha, s - \frac{\theta Q}{\alpha}, u + \frac{\eta_1 \nu M}{l_1\nu_0 + \nu M}$ and $-\nu_0$. Since one eigenvalue is always positive; therefore, S_1 is always unstable.

(ii) Two eigenvalues of $\hat{J}_{S_2}$ are $-(\alpha + \lambda_1 M)$, $\left(s + \xi M - \frac{\theta Q}{\alpha + \lambda_1 M}\right)$ and the other two eigenvalues are either negative or with negative real part. We note that one of the eigenvalue of $\hat{J}_{S_2}$ is $\left(s + \xi M - \frac{\theta Q}{\alpha + \lambda_1 M}\right)$, which is always positive if the condition (8) holds. Thus, S_2 is unstable whenever S^* exists.

(iii) From $\hat{J}_{S_3}$, we find that two of its eigenvalues are $u - \left(\phi - \frac{\phi_1 P_3}{k_1 + P_3}\right) N_3 + \frac{\eta_1 P_3}{l_1 + P_3}$ and $-\nu_0$ and the other two eigenvalues are roots of equation

$$\psi^2 + \left(\alpha + \frac{sN_3}{L}\right)\psi + \frac{\alpha s N_3}{L} + \lambda\theta N_3 = 0$$

which are either negative or with negative real part. Further $u - \left(\phi - \frac{\phi_1 P_3}{k_1+P_3}\right) N_3 + \frac{\eta_1 P_3}{l_1+P_3}$ is positive if the condition (7) holds. Thus S_3 is unstable whenever S^* exists.

(iv) The characteristic equation for $\hat{J}_{S^*}$ is given by

$$\psi^4 + D_1\psi^3 + D_2\psi^2 + D_3\psi + D_4 = 0, \tag{18}$$

where

$$\begin{aligned}
D_1 &= (\alpha + \lambda_1 B^*) + \frac{sN^*}{L} + \frac{uB^*}{M} + \nu_0,\\
D_2 &= \nu_0(\alpha + \lambda_1 B^*) + (\alpha + \lambda_1 B^* + \nu_0)\left(\frac{sN^*}{L} + \frac{uB^*}{M}\right) + \frac{sN^*}{L}\frac{uB^*}{M} +\\
&\quad \xi\left(\phi - \frac{\phi_1 P^*}{k_1 + P^*}\right) N^* B^* + \theta N^* \lambda + \nu\left(\frac{\phi_1 k_1 N^* B^*}{(k_1+P^*)^2} + \frac{\eta_1 l_1 B^*}{(l_1+P^*)^2}\right),\\
D_3 &= \nu_0(\alpha + \lambda_1 B^*)\left(\frac{sN^*}{L} + \frac{uB^*}{M}\right) + (\alpha + \lambda_1 B^* + \nu_0)\frac{sN^*}{L}\frac{uB^*}{M} +\\
&\quad \nu\left(\alpha + \lambda_1 B^* + \frac{sN^*}{L}\right)\left(\frac{\phi_1 k_1 N^* B^*}{(k_1+P^*)^2} + \frac{\eta_1 l_1 B^*}{(l_1+P^*)^2}\right) + \xi\left(\phi - \frac{\phi_1 P^*}{k_1+P^*}\right)\\
&\quad N^* B^*(\nu_0 + \alpha + \lambda_1 B^*) + \lambda_1\theta\left(\phi - \frac{\phi_1 P^*}{k_1+P^*}\right) N^* C^* B^* + \theta\lambda N^*\left(\nu_0 + \frac{uB^*}{M}\right),\\
D_4 &= \nu_0(\alpha + \lambda_1 B^*)\left\{\frac{sN^*}{L}\frac{uB^*}{M} + \xi N^* B^*\left(\phi - \frac{\phi_1 P^*}{k_1+P^*}\right)\right\} + \nu(\alpha + \lambda_1 B^*)\frac{sN^*}{L}\\
&\quad \left(\frac{\phi_1 k_1 N^* B^*}{(k_1+P^*)^2} + \frac{\eta_1 l_1 B^*}{(l_1+P^*)^2}\right) + \lambda_1\nu_0\theta\left(\phi - \frac{\phi_1 P^*}{k_1+P^*}\right) N^* B^* C^* +\\
&\quad \theta\lambda N^*\left\{\nu_0\frac{uB^*}{M} + \nu\left(\frac{\phi_1 k_1 N^* B^*}{(k_1+P^*)^2} + \frac{\eta_1 l_1 B^*}{(l_1+P^*)^2}\right)\right\}.
\end{aligned}$$

Here, it can be easily noted that all $D_i's (i = 1, 2, 3, 4)$ are positive. Using Routh–Hurwitz criterion, it is inferred that all the roots of equation (18) will lie in negative half of plane iff condition (17) is satisfied. □

3.3 Global stability analysis

Theorem 2 *The equilibrium S^*, if exists, is globally asymptotically stable in Γ provided the following conditions are satisfied:*

$$\lambda_1^2 C_m^2 < (\alpha + \lambda_1 B^*)\frac{\xi\lambda u}{M\theta\left(\phi - \frac{\phi_1 P^*}{k_1+P^*}\right)}, \tag{19}$$

$$\max\left\{\frac{\phi_1^2 N_m^2}{(k_1+P^*)^2}, \frac{\eta_1^2}{(l_1+P^*)^2}\right\} < \frac{1}{9}\frac{u^2\nu_0^2}{M^2\nu^2}. \tag{20}$$

Proof To prove the theorem, we define a positive definite function:

$$\begin{aligned}
V &= \frac{1}{2}(C - C^*)^2 + m_1\left(N - N^* - N^*\ln\frac{N}{N^*}\right) + m_2\left(B - B^* - B^*\ln\frac{B}{B^*}\right)\\
&\quad + \frac{m_3}{2}(P - P^*)^2,
\end{aligned} \tag{21}$$

where m_1, m_2 and m_3 are positive constants to be chosen appropriately.

The time derivative of V along the solution of system (5) is given as

$$\begin{aligned}\frac{dV}{dt} &= -(\alpha+\lambda_1 B^*)(C-C^*)^2 - \frac{m_1 s}{L}(N-N^*)^2 - \frac{m_2 u}{M}(B-B^*)^2 \\ &\quad -m_3\nu_0(P-P^*)^2 + (\lambda - m_1\theta)(C-C^*)(N-N^*) - \lambda_1 C(C-C^*)(B-B^*) \\ &\quad + \left\{m_1\xi - \left(\phi - \frac{\phi_1 P^*}{k_1+P^*}\right)m_2\right\}(B-B^*)(N-N^*) - m_3\nu(B-B^*)(P-P^*) \\ &\quad + \frac{m_2\phi_1 k_1 N}{(k_1+P)(k_1+P^*)}(B-B^*)(P-P^*) + \frac{m_2\eta_1 l_1}{(l_1+P)(l_1+P^*)}(B-B^*)(P-P^*).\end{aligned}$$

Choosing $m_1 = \frac{\lambda}{\theta}$ and $m_2 = \frac{\xi}{\left(\phi - \frac{\phi_1 P^*}{k_1+P^*}\right)} m_1 = \frac{\xi\lambda}{\theta\left(\phi - \frac{\phi_1 P^*}{k_1+P^*}\right)}$, we get

$$\begin{aligned}\frac{dV}{dt} &= -(\alpha+\lambda_1 B^*)(C-C^*)^2 - \frac{\lambda s}{L\theta}(N-N^*)^2 - \frac{\xi\lambda u}{M\theta\left(\phi - \frac{\phi_1 P^*}{k_1+P^*}\right)}(B-B^*)^2 \\ &\quad -m_3\nu_0(P-P^*)^2 - \lambda_1 C(C-C^*)(B-B^*) - m_3\nu(B-B^*)(P-P^*) \\ &\quad + \frac{\xi\lambda}{\theta\left(\phi - \frac{\phi_1 P^*}{k_1+P^*}\right)}\frac{\phi_1 k_1 N}{(k_1+P)(k_1+P^*)}(B-B^*)(P-P^*) \\ &\quad + \frac{\xi\lambda}{\theta\left(\phi - \frac{\phi_1 P^*}{k_1+P^*}\right)}\frac{\eta_1 l_1}{(l_1+P)(l_1+P^*)}(B-B^*)(P-P^*). \qquad (22)\end{aligned}$$

Thus, dV/dt is negative definite inside Γ if following inequalities hold:

$$\lambda_1^2 C_m^2 < (\alpha+\lambda_1 B^*)\frac{\xi\lambda u}{M\theta\left(\phi - \frac{\phi_1 P^*}{k_1+P^*}\right)}, \qquad (23)$$

$$m_3 < \frac{1}{3}\frac{\xi\lambda u\nu_0}{\nu^2 M\theta\left(\phi - \frac{\phi_1 P^*}{k_1+P^*}\right)}, \qquad (24)$$

$$m_3 > \frac{3M\xi\lambda\phi_1^2 N_m^2}{u\nu_0\theta(k_1+P^*)^2\left(\phi - \frac{\phi_1 P^*}{k_1+P^*}\right)}, \qquad (25)$$

$$m_3 > \frac{3M\xi\lambda\eta_1^2}{u\nu_0\theta(l_1+P^*)^2\left(\phi - \frac{\phi_1 P^*}{k_1+P^*}\right)}. \qquad (26)$$

From above inequalities (24)–(26), we can choose $m_3 > 0$ provided condition (20) holds. Thus dV/dt is negative definite in Γ provided conditions (19) and (20) are satisfied. Hence the proof. □

3.4 Hopf-bifurcation analysis

In this section, we examine the criterion under which the system (5) undergoes Hopf-bifurcation at interior equilibrium $S^*(C^*, N^*, B^*, P^*)$ by taking ϕ as bifurcation parameter.

Theorem 3 *The model system* (5) *undergoes Hopf-bifurcation about the interior equilibrium* S^* *iff there exists* $\phi = \phi_c$ *such that*

$$\begin{aligned} &(i)\ \ D_3(\phi_c)(D_1(\phi_c)D_2(\phi_c) - D_3(\phi_c)) - D_1^2(\phi_c)D_4(\phi_c) = 0, \\ &(ii)\ \left[\frac{d}{d\phi}(D_1D_2D_3 - D_3^2 - D_1^2D_4)\right]_{\phi=\phi_c} \neq 0. \end{aligned} \tag{27}$$

Proof The characteristic equation (18) can be written as

$$\psi^4 + D_1(\phi)\psi^3 + D_2(\phi)\psi^2 + D_3(\phi)\psi + D_4(\phi) = 0. \tag{28}$$

Let at $\phi = \phi_c$,

$$D_3(\phi_c)(D_1(\phi_c)D_2(\phi_c) - D_3(\phi_c)) - D_1^2(\phi_c)D_4(\phi_c) = 0.$$

Then, at $\phi = \phi_c$, the characteristic equation can be written as

$$\left(\psi^2 + \frac{D_3}{D_1}\right)\left(\psi^2 + D_1\psi + \frac{D_1D_4}{D_3}\right) = 0. \tag{29}$$

Above equation has four roots, say ψ_i $(i = 1, 2, 3, 4)$, with a pair of purely imaginary roots $\psi_{1,2} = \pm i\omega_0$ where $\omega_0 = (D_3/D_1)^{1/2}$.

For existence of Hopf-bifurcation, the root other than $\pm i\omega_0$(i.e., ψ_3 and ψ_4) should have negative real parts. To identify the nature of remaining two roots, we have

$$\psi_3 + \psi_4 = -D_1, \tag{30}$$

$$\omega_0^2 + \psi_3\psi_4 = D_2, \tag{31}$$

$$\omega_0^2(\psi_3 + \psi_4) = -D_3, \tag{32}$$

$$\omega_0^2\psi_3\psi_4 = D_4. \tag{33}$$

If ψ_3 and ψ_4 are complex conjugate, then from equation (30), we have $2\Re(\psi_3) = -D_1$ i.e., ψ_3 and ψ_4 have negative real parts. If ψ_3 and ψ_4 are real roots, then equations (30) and (33) yield that ψ_3 and ψ_4 are negative. Thus the roots ψ_3 and ψ_4 are either negative or with negative real part. Now, we will find out the transversality condition under which Hopf-bifurcation occurs at S^*. Let at any point $\phi \in (\phi_c - \epsilon, \phi_c + \epsilon)$, $\psi_{1,2} = \kappa(\phi) \pm i\rho(\phi)$. Substituting this in equation (28), we get

$$\kappa^4 + D_1\kappa^3 + D_2\kappa^2 + D_3\kappa + D_4 + \rho^4 - 6\kappa^2\rho^2 - 3D_1\kappa\rho^2 - D_2\rho^2 = 0 \tag{34}$$

and

$$4\kappa\rho(\kappa^2 - \rho^2) - D_1\rho^3 + 3D_1\kappa^2\rho + 2D_2\kappa\rho + D_3\rho = 0. \tag{35}$$

As $\rho(\phi) \neq 0$, from equation (35), we get

$$-(4\kappa + D_1)\rho^2 + 4\kappa^3 + 3D_1\kappa^2 + 2D_2\kappa + D_3 = 0.$$

Substituting this in equation (34) and differentiating with respect to ϕ and using the fact that $\kappa(\phi_c) = 0$, we have

$$\left[\frac{d\kappa}{d\phi}\right]_{\phi=\phi_c} = \left[\frac{\frac{d}{d\phi}(D_1D_2D_3 - D_3^2 - D_1^2D_4)}{-2D_1(D_1D_3 + (2D_3/D_1 - D_2)^2)}\right]_{\phi=\phi_c} \neq 0$$

if

$$\left[\frac{d}{d\phi}(D_1D_2D_3 - D_3^2 - D_1^2D_4)\right]_{\phi=\phi_c} \neq 0. \tag{36}$$

The inequality (36) gives the transversality condition. □

3.5 Stability and direction of Hopf-bifurcation

We shift the origin to S^* by applying the transformation

$$z_1 = C - C^*,\ z_2 = N - N^*,\ z_3 = B - B^*,\ z_4 = P - P^*$$

on the model system (5) and obtain the following system

$$\dot{Z} = \hat{J}_{S^*}Z + G(Z), \tag{37}$$

where

$$Z = \begin{pmatrix} z_1 \\ z_2 \\ z_3 \\ z_4 \end{pmatrix},\ \hat{J}_{S^*} = \begin{pmatrix} -(\alpha+\lambda_1 B^*) & \lambda & -\lambda_1 C^* & 0 \\ -\theta N^* & \frac{-sN^*}{L} & \xi N^* & 0 \\ 0 & -\left(\phi - \frac{\phi_1 P^*}{k_1+P^*}\right)B^* & \frac{-uB^*}{M} & \frac{\phi_1 k_1 N^* B^*}{(k_1+P^*)^2} + \frac{\eta_1 l_1 B^*}{(l_1+P^*)^2} \\ 0 & 0 & -\nu & -\nu_0 \end{pmatrix}.$$

and

$$G = \begin{pmatrix} g_1 \\ g_2 \\ g_3 \\ g_4 \end{pmatrix} = \begin{pmatrix} -\lambda_1 z_1 z_3 \\ \frac{-s}{L}z_2^2 + \xi z_2 z_3 - \theta z_1 z_2 \\ \frac{-u}{M}z_3^2 - d_1 z_2 z_3 + d_2 z_2 z_4 + d_3 z_3 z_4 - d_4 z_4^2 \\ 0 \end{pmatrix}.$$

where, $d_1 = \left(\phi - \frac{\phi_1 P^*}{k_1+P^*}\right)$, $d_2 = \frac{\phi_1 k_1 B^*}{(k_1+P^*)^2}$, $d_3 = \frac{\eta_1 l_1}{(l_1+P^*)^2} + \frac{\phi_1 k_1 N^*}{(k_1+P^*)^2}$, $d_4 = \frac{\phi_1 k_1 N^* B^*}{(k_1+P^*)^3} + \frac{\eta_1 B^*}{(l_1+P^*)^2} - \frac{\eta_1 P^* B^*}{(l_1+P^*)^3}$.

The eigenvectors v_1, v_2 and v_3 of Jacobian matrix $\hat{J}_{S^*}$ corresponding the eigenvalues $i\omega_0$, ψ_3 and ψ_4, respectively, at $\phi = \phi_c$ are given as

$$v_1 = \begin{pmatrix} a_{11} - ia_{12} \\ a_{21} - ia_{22} \\ a_{31} - ia_{32} \\ a_{41} - ia_{42} \end{pmatrix},\ v_2 = \begin{pmatrix} a_{13} \\ a_{23} \\ a_{33} \\ a_{43} \end{pmatrix} \text{ and } v_3 = \begin{pmatrix} a_{14} \\ a_{24} \\ a_{34} \\ a_{44} \end{pmatrix},$$

where

$$a_{11} = \nu_0\left(\lambda\xi N^* - \frac{\lambda_1 s}{L}C^*N^*\right) + \omega_0^2\lambda_1 C^*,\ a_{12} = -\omega_0\left(\lambda\xi N^* - \frac{\lambda_1 s}{L}C^*N^* - \nu_0\lambda_1 C^*\right),$$
$$a_{21} = \nu_0\left[(\alpha+\lambda_1 B^*)\xi N^* + \theta\lambda_1 C^*N^*\right] - \omega_0^2\xi N^*,$$
$$a_{22} = -\omega_0\left[(\alpha+\lambda_1 B^*)\xi N^* + \theta\lambda_1 C^*N^* + \nu_0\xi N^*\right],$$
$$a_{31} = \nu_0\left[\theta\lambda N^* + (\alpha+\lambda_1 B^*)\frac{sN^*}{L} - \omega_0^2\right] - \omega_0^2\left(\alpha+\lambda_1 B^* + \frac{sN^*}{L}\right),$$
$$a_{32} = -\omega_0\left[\theta\lambda N^* + (\alpha+\lambda_1 B^*)\frac{sN^*}{L} - \omega_0^2 + \nu_0\left(\alpha+\lambda_1 B^* + \frac{sN^*}{L}\right)\right],$$

$$a_{41} = -\nu\left[\theta\lambda N^* + (\alpha + \lambda_1 B^*)\frac{sN^*}{L} - \omega_0^2\right],\ a_{42} = \omega_0\nu\left(\alpha + \lambda_1 B^* + \frac{sN^*}{L}\right),$$
$$a_{13} = (v_0 + \psi_3)\left[\lambda\xi N^* - \lambda_1 C^*\left(\frac{sN^*}{L} + \psi_3\right)\right],$$
$$a_{23} = (v_0 + \psi_3)\left[(\alpha + \lambda_1 B^* + \psi_3)\xi N^* + \theta\lambda_1 C^* N^*\right],$$
$$a_{33} = (v_0 + \psi_3)\left[\theta\lambda N^* + (\alpha + \lambda_1 B^* + \psi_3)\left(\frac{sN^*}{L} + \psi_3\right)\right],$$
$$a_{43} = -\nu\left[\theta\lambda N^* + (\alpha + \lambda_1 B^* + \psi_3)\left(\frac{sN^*}{L} + \psi_3\right)\right],$$
$$a_{14} = (v_0 + \psi_4)\left[\lambda\xi N^* - \lambda_1 C^*\left(\frac{sN^*}{L} + \psi_4\right)\right],$$
$$a_{24} = (v_0 + \psi_4)\left[(\alpha + \lambda_1 B^* + \psi_4)\xi N^* + \theta\lambda_1 C^* N^*\right],$$
$$a_{34} = (v_0 + \psi_4)\left[\theta\lambda N^* + (\alpha + \lambda_1 B^* + \psi_4)\left(\frac{sN^*}{L} + \psi_4\right)\right],$$
$$a_{44} = -\nu\left[\theta\lambda N^* + (\alpha + \lambda_1 B^* + \psi_4)\left(\frac{sN^*}{L} + \psi_4\right)\right].$$

Define

$$A = (\Re(v_1), -\Im(v_1), v_2, v_3) = \begin{pmatrix} a_{11} & a_{12} & a_{13} & a_{14} \\ a_{21} & a_{22} & a_{23} & a_{24} \\ a_{31} & a_{32} & a_{33} & a_{34} \\ a_{41} & a_{42} & a_{43} & a_{44} \end{pmatrix}.$$

Matrix A is a nonsingular matrix such that

$$A^{-1}\hat{J}_{S^*}A = \begin{pmatrix} 0 & -\omega_0 & 0 & 0 \\ \omega_0 & 0 & 0 & 0 \\ 0 & 0 & \psi_3 & 0 \\ 0 & 0 & 0 & \psi_4 \end{pmatrix}.$$

Let the inverse of matrix A is given by

$$A^{-1} = \begin{pmatrix} q_{11} & q_{12} & q_{13} & q_{14} \\ q_{21} & q_{22} & q_{23} & q_{24} \\ q_{31} & q_{32} & q_{33} & q_{34} \\ q_{41} & q_{42} & q_{43} & q_{44} \end{pmatrix}.$$

Let $Z = AY$ or $Y = A^{-1}Z$, where $Y = (y_1, y_2, y_3, y_4)^T$. Under this linear transformation system (37) becomes

$$\dot{Y} = (A^{-1}\hat{J}_{S^*}A)Y + \hat{F}(Y) \tag{38}$$

where, $\hat{F}(Y) = A^{-1}G(AY)$,

This can be written as

$$\dot{y_1} = -\omega_0 y_2 + F_1(y_1, y_2, y_3, y_4) \tag{39}$$
$$\dot{y_2} = \omega_0 y_1 + F_2(y_1, y_2, y_3, y_4) \tag{40}$$
$$\dot{y_3} = \psi_3 y_3 + F_3(y_1, y_2, y_3, y_4) \tag{41}$$

$$\dot{y_4} = \psi_4 y_4 + F_4(y_1, y_2, y_3, y_4) \tag{42}$$

where $\hat{F} = (F_1, F_2, F_3, F_4)^T$,

$$\begin{aligned}
F_1 &= q_{11}g_1 + q_{12}g_2 + q_{13}g_3 + q_{14}g_4,\\
F_2 &= q_{21}g_1 + q_{22}g_2 + q_{23}g_3 + q_{24}g_4,\\
F_3 &= q_{31}g_1 + q_{32}g_2 + q_{33}g_3 + q_{34}g_4,\\
F_4 &= q_{41}g_1 + q_{42}g_2 + q_{43}g_3 + q_{44}g_4,\\
g_1 &= -\lambda_1(a_{11}y_1 + a_{12}y_2 + a_{13}y_3 + a_{14}y_4)(a_{31}y_1 + a_{32}y_2 + a_{33}y_3 + a_{34}y_4),\\
g_2 &= -\frac{s}{L}(a_{21}y_1 + a_{22}y_2 + a_{23}y_3 + a_{24}y_4)^2\\
&\quad +\xi(a_{21}y_1 + a_{22}y_2 + a_{23}y_3 + a_{24}y_4)(a_{31}y_1 + a_{32}y_2 + a_{33}y_3 + a_{34}y_4)\\
&\quad -\theta(a_{11}y_1 + a_{12}y_2 + a_{13}y_3 + a_{14}y_4)(a_{21}y_1 + a_{22}y_2 + a_{23}y_3 + a_{24}y_4),\\
g_3 &= -\frac{u}{M}(a_{31}y_1 + a_{32}y_2 + a_{33}y_3 + a_{34}y_4)^2\\
&\quad -\left(\phi - \frac{\phi_1 P^*}{k_1 + P^*}\right)(a_{21}y_1 + a_{22}y_2 + a_{23}y_3 + a_{24}y_4)(a_{31}y_1 + a_{32}y_2 + a_{33}y_3 + a_{34}y_4)\\
&\quad +\left[\frac{\phi_1 k_1 B^*}{(k_1 + P^*)^2}\right](a_{21}y_1 + a_{22}y_2 + a_{23}y_3 + a_{24}y_4)(a_{41}y_1 + a_{42}y_2 + a_{43}y_3 + a_{44}y_4)\\
&\quad +\left[\frac{\eta_1 l_1}{(l_1 + P^*)^2} + \frac{\phi_1 k_1 N^*}{(k_1 + P^*)^2}\right](a_{31}y_1 + a_{32}y_2 + a_{33}y_3 + a_{34}y_4)\\
&\quad \times(a_{41}y_1 + a_{42}y_2 + a_{43}y_3 + a_{44}y_4)\\
&\quad -\left[\frac{\phi_1 k_1 N^* B^*}{(k_1 + P^*)^3} + \frac{\eta_1 B^*}{(l_1 + P^*)^2} - \frac{\eta_1 P^* B^*}{(l_1 + P^*)^3}\right](a_{41}y_1 + a_{42}y_2 + a_{43}y_3 + a_{44}y_4)^2,\\
g_4 &= 0.
\end{aligned}$$

Furthermore, we can calculate g_{11}, g_{02}, g_{20}, G_{21}, G^1_{110}, G^2_{110}, G^1_{101}, G^2_{101}, ω^1_{11}, ω^2_{11}, ω^1_{20}, ω^2_{20} following the procedure given in Hassard et al. (1981).

Now, we have

$$g_{21} = G_{21} + 2(G^1_{110}\omega^1_{11} + G^2_{110}\omega^2_{11}) + G^1_{101}\omega^1_{20} + G^2_{101}\omega^2_{20}. \tag{43}$$

$$c_1(0) = \frac{i}{2\omega_0}\left(g_{11}g_{20} - 2|g_{11}|^2 - \frac{|g_{02}|^2}{3}\right) + \frac{g_{21}}{2}, \tag{44}$$

$$\mu_2 = -\frac{\Re c_1(0)}{\gamma'(0)} \tag{45}$$

$$\tau_2 = -\frac{\Im c_1(0) + \mu_2\omega'(0)}{\omega_0} \tag{46}$$

$$\beta_2 = -2\mu_2\gamma'(0), \tag{47}$$

where $\gamma'(0) = \frac{d}{d\phi}(\Re\psi_1(\phi))|_{\phi=\phi_c}$ and $\omega'(0) = \frac{d}{d\phi}(\Im\psi_1(\phi))|_{\phi=\phi_c}$.

Theorem 4 *The Hopf-bifurcation occurring at $\phi = \phi_c$ about S^* is supercritical or subcritical according as $\mu_2 > 0$ or $\mu_2 < 0$ and the bifurcating periodic solutions exist for $\phi > \phi_c$ or $\phi < \phi_c$. The periodic orbits are stable or unstable according to $\beta_2 < 0$ or $\beta_2 > 0$ and the period of orbits increases or decreases depending on $\tau_2 > 0$ or $\tau_2 < 0$.*

4 The optimal control problem

The execution cost of forest management programs restricts their implementation on large scale. Thus, the policymakers sought management policies that reduce the CO_2 emission at minimum implementation cost. The optimal control theory can be effectively used to design the cost effective forest management policies. For this purpose, we modify the model system (5) by taking a Lebesgue measurable function $v(t)$ as the increased execution rate of forest management programs, on some finite time interval $[0, t_f]$. With this assumption, the model system (5) can be rewritten as

$$\begin{aligned}
\dot{C} &= Q + \lambda N - \alpha C - \lambda_1 BC,\\
\dot{N} &= sN\left(1 - \frac{N}{L}\right) + \xi NB - \theta CN,\\
\dot{B} &= uB\left(1 - \frac{B}{M}\right) - \left(\phi - \frac{\phi_1 P}{k_1 + P}\right)NB + \frac{\eta_1 PB}{l_1 + P},\\
\dot{P} &= (v + v(t))(M - B) - \nu_0 P,
\end{aligned} \tag{48}$$

where

$$C(0) = C_0 > 0,\ N(0) = N_0 \geq 0,\ B(0) = B_0 \geq 0,\ P(0) = P_0 \geq 0. \tag{49}$$

Our problem is to minimize the cost functional

$$J = \int_0^{t_f} [w_1 C(t) + w_2 v^2(t)]dt, \tag{50}$$

subject to the system (48) with initial conditions (49). In the objective functional, the coefficients w_1 and w_2 are the weight parameters balancing the effect of both the terms in the objective functional. The first term in the cost functional represents the cost for carbon dioxide mitigation, and the second term represents the cost associated with the implementation of forest management programs. The quadratic expression of control shows the nonlinear cost arising at a high implementation level. We seek optimal control $v^*(t)$ such that

$$J(v^*(t)) = \min_{v(t)\in U} J(v(t)), \tag{51}$$

where $U = \left\{v(t) : v(t) \text{ is measurable }, 0 \leq v(t) \leq v_{\max}, t \in [0, t_f]\right\}$ is the control set.

Theorem 5 *There exists an optimal control v^* such that $J(v^*(t)) = \min_{v(t)\in U} J(v(t))$, subject to system (48) with initial conditions (49).*

Proof The boundedness of the solutions of the system (48) assures the existence of solution to the control system using the result in Lukes (1982). Thus, it can be concluded that the set of controls and corresponding state variables is non-empty. It can be seen that the set U is closed. Further, U is convex and the integrand $w_1 C(t) + w_2 v^2(t)$ of the cost functional (50) is convex on U. Using the boundedness of solutions, it can be deduced that the right-hand side of system (48) is bounded by a linear function of control and state variables. In addition, the integrand of functional (50) satisfies the following inequality:

$$w_1 C(t) + w_2 v^2(t) \geq c_1(|v(t)|)^\rho - c_2, \tag{52}$$

for some $c_1, c_2 > 0$ and $\rho > 1$. The above arguments prove the existence of optimal control v^* following the results from Fleming and Rishel (1975). □

The optimal control is characterized using Pontryagin's maximum principle. The Hamiltonian H is given by

$$\begin{aligned} H(C,N,B,P,v,\nu_1,\nu_2,\nu_3,\nu_4) = {} & w_1C(t)+w_2v^2(t) \\ & +\nu_1(Q+\lambda N-\alpha C-\lambda_1 BC) \\ & +\nu_2\left\{sN\left(1-\frac{N}{L}\right)+\xi NB-\theta CN\right\} \\ & +\nu_3\left\{uB\left(1-\frac{B}{M}\right)-\left(\phi-\frac{\phi_1 P}{k_1+P}\right)NB+\frac{\eta_1 PB}{l_1+P}\right\} \\ & +\nu_4((\nu+v(t))(M-B)-\nu_0 P), \end{aligned} \tag{53}$$

where $\nu_i (i = 1, 2, 3, 4)$ are the adjoint variables. The adjoint variables satisfy the following equations:

$$\begin{aligned} \dot{\nu_1} &= -\frac{\partial H}{\partial C} = -w_1+(\alpha+\lambda_1 B)\nu_1+\theta N\nu_2, \\ \dot{\nu_2} &= -\frac{\partial H}{\partial N} = -\nu_1\lambda-\nu_2\left\{s\left(1-\frac{2N}{L}\right)+\xi B-\theta C\right\}+\nu_3 B\left(\phi-\frac{\phi_1 P}{k_1+P}\right), \\ \dot{\nu_3} &= -\frac{\partial H}{\partial B} = \nu_1\lambda_1 C-\xi N\nu_2-\nu_3\left\{u\left(1-\frac{2B}{M}\right)\right. \\ &\quad \left.-\left(\phi-\frac{\phi_1 P}{k_1+P}\right)N+\frac{\eta_1 P}{l_1+P}\right\}+\nu_4(\nu+v(t)), \\ \dot{\nu_4} &= -\frac{\partial H}{\partial P} = -\nu_3\left\{\frac{\phi_1 k_1 NB}{(k_1+P)^2}+\frac{\eta_1 l_1 B}{(l_1+P)^2}\right\}+\nu_4\nu_0. \end{aligned} \tag{54}$$

The transversality conditions are

$$\nu_1(t_f)=\nu_2(t_f)=\nu_3(t_f)=\nu_4(t_f)=0. \tag{55}$$

With the help of the optimality condition, i.e., $\frac{\partial H}{\partial v}=0$ at $v=v^*$, we get $v^*=-\frac{\nu_4(M-B)}{2w_2}$. Taking into account the bound constraints for control, we get

$$v^*=\begin{cases} 0, & \text{if } \dfrac{-\nu_4(M-B)}{2w_2}\le 0, \\ \dfrac{-\nu_4(M-B)}{2w_2}, & \text{if } 0<\dfrac{-\nu_4(M-B)}{2w_2}<v_{\max}, \\ v_{\max}, & \text{if } \dfrac{-\nu_4(M-B)}{2w_2}\ge v_{\max}. \end{cases}$$

Thus, the characterization of optimal control v^*, which minimizes J subjected to the state system (48) over the set U, is given by

$$v^*(t)=\max\left\{\min\left(-\frac{\nu_4(M-B)}{2w_2},v_{\max}\right),0\right\}. \tag{56}$$

The optimality system comprises of the state system (48), the adjoint system (54) with optimal control (56), and conditions (49) and (55).

5 Numerical simulation

To depict the effect of deforestation and forest management programs on the dynamics of atmospheric carbon dioxide, the numerical simulations are performed for the set of parameter values given in Table 1. For these parameter values, the eigenvalues of $\hat{J}_{S^*}$ are $-0.02613526 \pm 0.01840753\, i$ and $-0.08977696 \pm 0.01470386\, i$, which lie in the left half of the complex plane, inferring the local asymptotic stability of S^*. Figure 1 depicts the global stability of S^* in $C-N-B$ and $C-B-P$ spaces. We may see that the solution trajectories of system (5) with different initial starts are approaching the equilibrium values. Figure 2 shows the effect of changes in the deforestation rate ϕ on the time evolutions of CO_2 and forest biomass. It can be seen that as the deforestation rate ϕ increases, the CO_2 level increases and that of forest biomass decreases. Figure 3 depicts that an increase in the implementation rate of forest management programs causes an increase in the equilibrium level of forest biomass and a decrease in that of CO_2.

To show the effect of changes in the maximum efficacy of forest management programs to reduce the deforestation rate, i.e., ϕ_1 and half-saturation constant k_1 on equilibrium levels of $C(t)$ and $B(t)$, we have plotted the contour plots of equilibrium levels of CO_2 and forest biomass as a function of ϕ_1 and k_1 in Fig. 4. From this figure, we observe that the equilibrium level of CO_2 declines with an increase in the value of ϕ_1 and a decrease in the value of k_1. The equilibrium level of forest biomass increases with an increase in the value of ϕ_1 and a decrease in the value of k_1. It should be noted that the low values of k_1 represent those forest management programs where reduction in deforestation rate caused by forest management programs increases more rapidly at low values of $P(t)$. Figure 4 clearly shows that for low values of k_1, an increase in maximum efficiency of management programs to

Table 1 Parameter values for system (5)

Parameter	Value	Unit	Source
Q	1	ppm month^{-1}	(Misra and Verma 2013)
λ	0.05	ppm (person month)$^{-1}$	(Misra and Verma 2013)
α	0.003	$(month)^{-1}$	(Misra and Verma 2013)
λ_1	0.0001	(ton month)$^{-1}$	(Misra and Verma 2013)
s	0.01	month^{-1}	(Misra and Verma 2013)
L	1000	Person	(Misra and Verma 2013)
ξ	0.0000002	(ton month)$^{-1}$	Assumed
θ	0.00001	(ppm month)$^{-1}$	(Misra and Verma 2013)
u	0.2	month^{-1}	(Misra and Verma 2013)
M	2000	ton	(Misra and Verma 2013)
ϕ_1	0.00007	(person month)$^{-1}$	Assumed
k_1	100	Million dollar	Assumed
l_1	50	Million dollar	Assumed
η_1	0.01	month^{-1}	Assumed
ν	0.01	Million dollar(ton month)$^{-1}$	Assumed
ν_0	0.1	(month)$^{-1}$	Assumed
ϕ	0.0003	(person month)$^{-1}$	Assumed

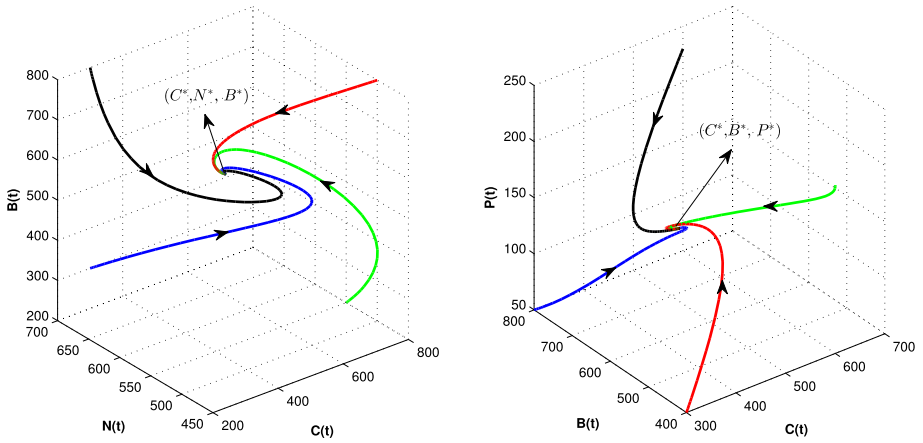

Fig. 1 Global stability of S^* in $C - N - B$ space and $C - B - P$ space

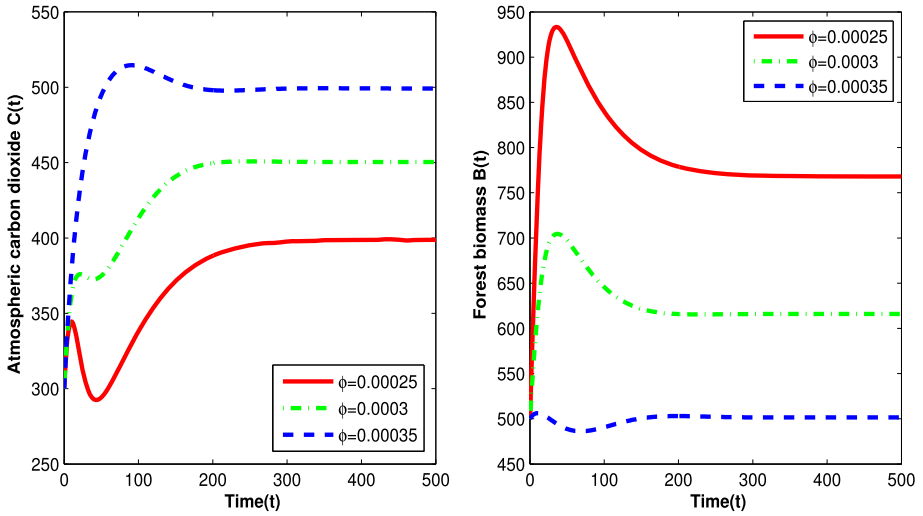

Fig. 2 Time evolution of atmospheric carbon dioxide and forest biomass for different values of ϕ. The other parameter values are same as in Table 1

reduce deforestation rate ϕ_1 causes more increase in forest biomass and consequently more decline in CO_2 level. Figure 5 depicts the contour plots of equilibrium levels of CO_2 and forest biomass as a function of the maximum efficiency of forest management programs to increase forest biomass η_1 and half saturation constant l_1. From this figure, we can observe that the equilibrium level of CO_2 declines with an increase in the value of η_1 and a decrease in the value of l_1. The equilibrium level of forest biomass increases with an increase in the value of η_1 and a decrease in the value of l_1. It should be noted that the low values of l_1 represent those forest management programs where increase in forest biomass caused by forest management programs increases more rapidly at low values of $P(t)$. Figure 5 clearly shows that for low values of l_1, an increase in maximum efficiency of forest management programs to increase the forest biomass η_1 causes more increase in forest biomass and consequently more decline

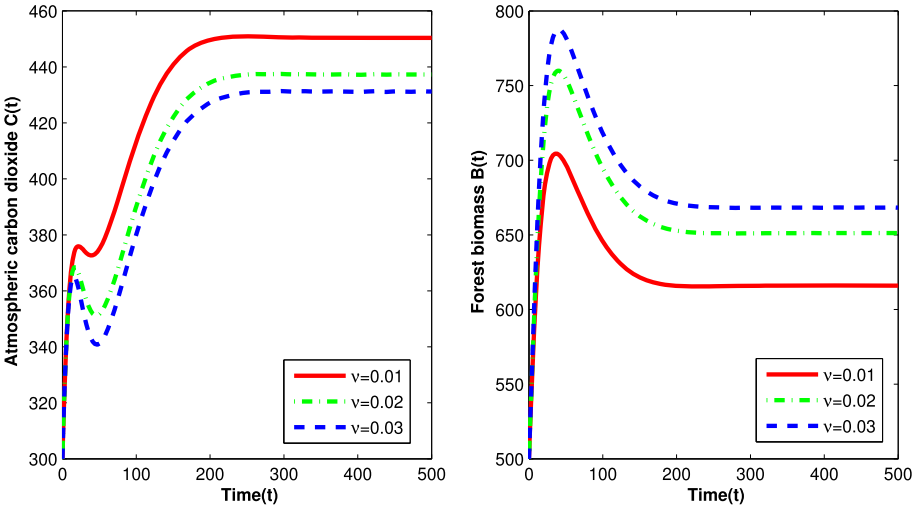

Fig. 3 Time evolution of atmospheric carbon dioxide and forest biomass for different values of ν. The other parameter values are same as in Table 1

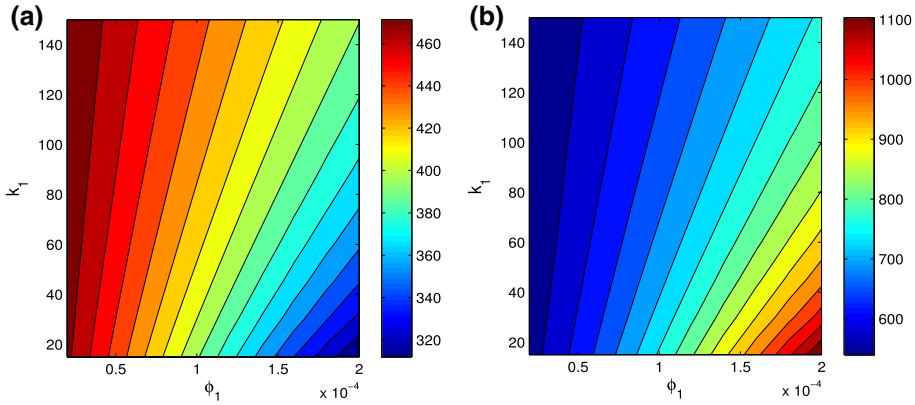

Fig. 4 Contour plots of equilibrium levels of **a** atmospheric carbon dioxide and **b** forest biomass as a function of ϕ_1 and k_1

in CO_2 level. Figure 6 presents a comparison between the time variations in atmospheric CO_2 and forest biomass when effect of forest management programs is not considered ($\phi_1 = 0,\ \eta_1 = 0$), when forest management programs contain only those strategies which increase forest biomass ($\phi_1 = 0,\ \eta_1 = 0.01$), when forest management programs contain only those strategies which focus on reducing deforestation rate ($\phi_1 = 0.00007,\ \eta_1 = 0$), and when forest management programs comprise of both kinds of strategies ($\phi_1 = 0.00007,\ \eta_1 = 0.01$). This figure shows that in absence of forest management programs, the equilibrium level of CO_2 settles to a high level and forest biomass settles to low level in comparison to the cases when forest management programs are applied. The reduction bring in the equilibrium CO_2 level by forest management programs is least when management programs contain only those strategies which increase forest biomass ($\phi_1 = 0,\ \eta_1 = 0.01$) and highest when it comprise of both kinds of strategies ($\phi_1 = 0.00007,\ \eta_1 = 0.01$).

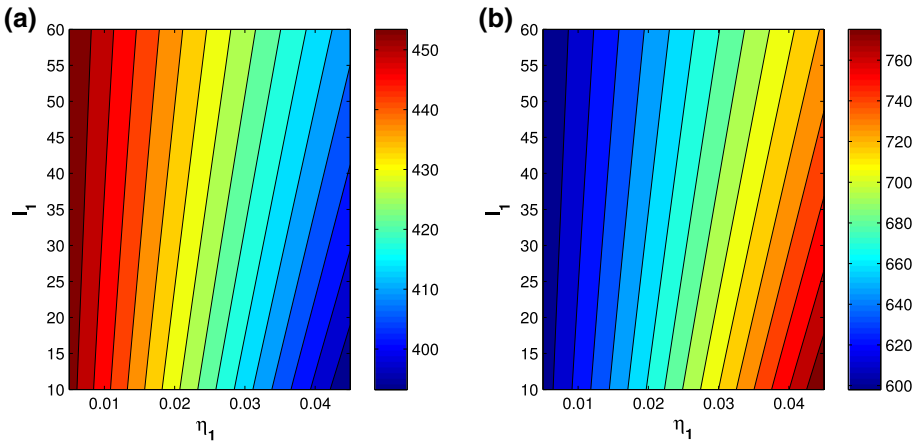

Fig. 5 Contour plots of equilibrium levels of **a** atmospheric carbon dioxide and **b** forest biomass as a function of η_1 and l_1

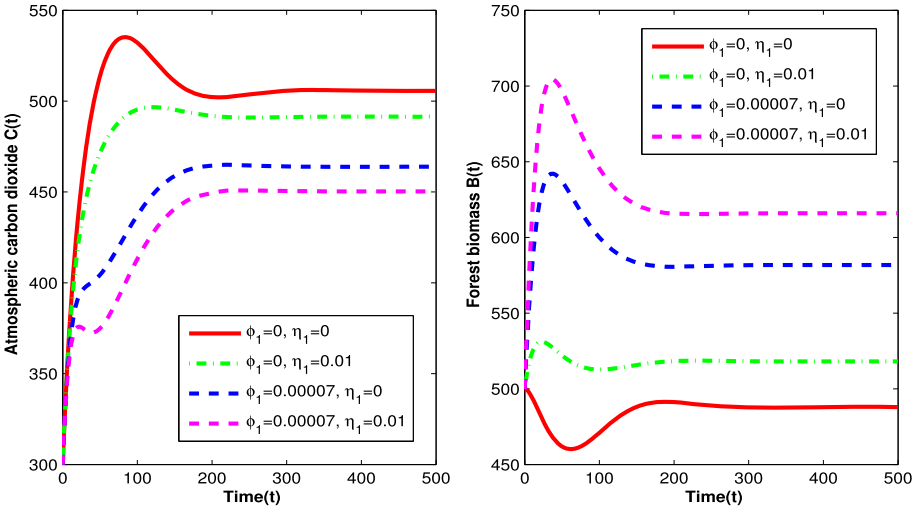

Fig. 6 Time evolution of atmospheric carbon dioxide and forest biomass for different values of ϕ_1 and η_1. The other parameter values are same as in Table 1

The dynamics of the system (5) about interior equilibrium S^* changes with an increase in the deforestation rate parameter 'ϕ'. For small values of ϕ, S^* is stable while an increase in ϕ above a critical value destabilizes the equilibrium S^* and periodic solutions arise via Hopf-bifurcation. The critical value of ϕ at which stability loss occurs via Hopf-bifurcation has been calculated for the set of parameter values given in Table 1 and is found to be $\phi_c = 0.0007067$. It is found that for $\phi \in [0, \phi_c)$, all the eigenvalues of the Jacobian $\hat{J}_{S^*}$ lies in the left half of the complex plane showing that the equilibrium S^* is stable while for $\phi > \phi_c$, S^* loses stability and becomes unstable. Further, the computations of μ_2, τ_2 and β_2 show that $\mu_2 > 0$, $\tau_2 > 0$ and $\beta_2 < 0$ at $\phi = \phi_c$. Using theorem 4, this can be inferred that supercritical Hopf-bifurcation occurs at $\phi = \phi_c$ yielding a family of stable periodic solutions with increasing time period. Figures 7 and 8 show the time variations of atmospheric CO_2 concentration

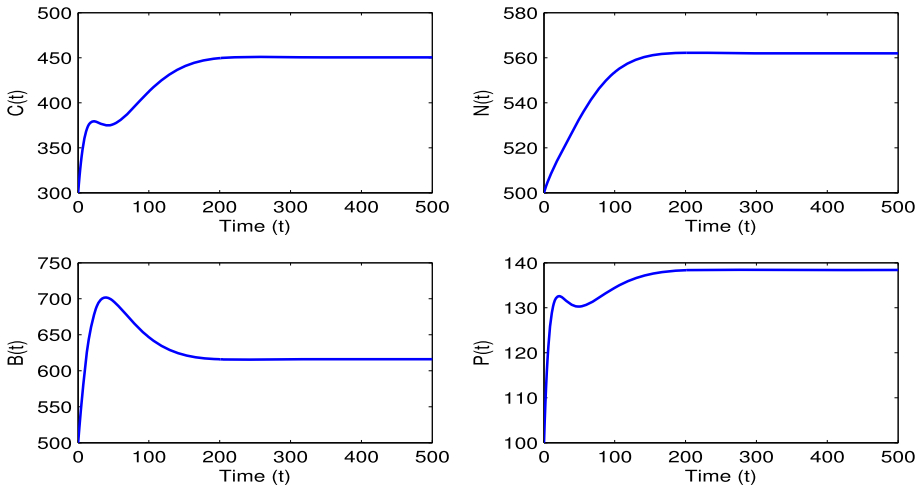

Fig. 7 Time evolution of C, N, B and P for $\phi = 0.0003$. The other parameter values are same as in Table 1

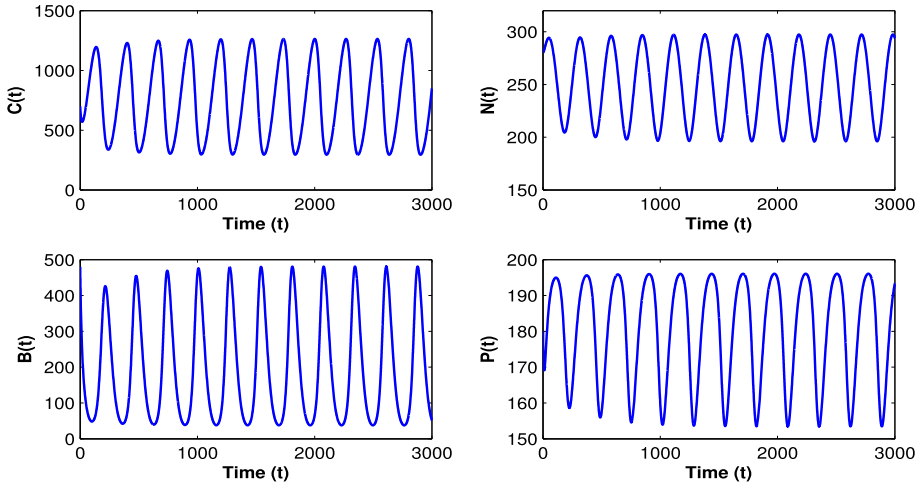

Fig. 8 Time evolution of C, N, B and P for $\phi = 0.0008$. The other parameter values are same as in Table 1

$C(t)$, human population $N(t)$, forest biomass $B(t)$ and forest management programs $P(t)$ for $\phi = 0.0003(< \phi_c)$ and $\phi = 0.0008(> \phi_c)$, respectively. These diagrams reveal that for $\phi \in [0, \phi_c)$, all the variables settle down to their equilibrium values but for $\phi > \phi_c$, all the variables show oscillatory behaviour. This shows that an increase in deforestation rate above the threshold value ϕ_c may destabilize the interior equilibrium and sustained oscillation may arise. These oscillations may dampen gradually and eventually die out with an increase in the maximum efficiency of forest management programs to reduce the deforestation rate, i.e. ϕ_1. To show this effect of increase in ϕ_1 on system dynamics, we have plotted the time variations of $C(t)$, $N(t)$, $B(t)$ and $P(t)$ for $\phi = 0.0008$ and $\phi_1 = 0.0003$ in Fig. 9. From this figure, it can be seen that all variables attain the equilibrium levels for $\phi = 0.0008$ and $\phi_1 = 0.0003$.

To get a more clear picture, we have drawn a bifurcation diagram of the system (5) by taking ϕ as a bifurcation parameter in Fig. 10. This figure shows that for small values of

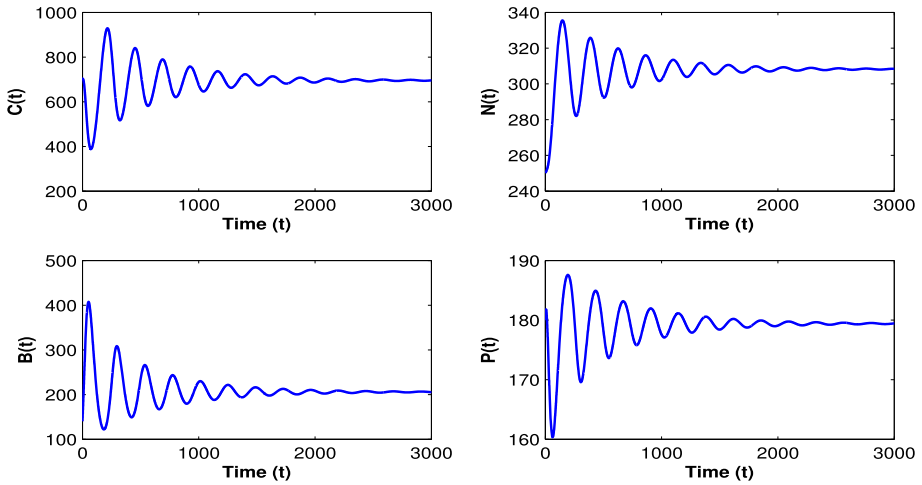

Fig. 9 Time evolution of C, N, B and P for ϕ=0.0008 and $\phi_1 = 0.0003$. The other parameter values are same as in Table 1

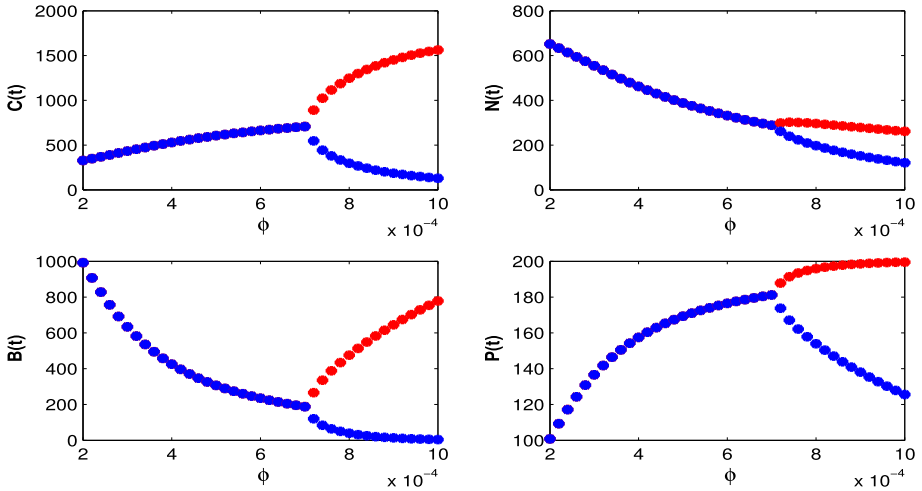

Fig. 10 Bifurcation diagrams of atmospheric carbon dioxide, human population, forest biomass and forest management programs with respect to ϕ. The other parameters take same values as in Table 1

ϕ, all the variables approach their equilibrium values. However, as the deforestation rate ϕ crosses the Hopf-bifurcation threshold ϕ_c, interior equilibrium losses stability and sustained oscillations of increasing amplitude are observed. Further, for $\phi = 0.0008$, if we increase the value of ϕ_1, then the amplitude of the period of oscillation decreases, and beyond a critical value of ϕ_1, the periodic oscillation dies out and the system gets stabilized (see Fig. 11). The same dynamic behavior is observed when the value of η_1 is increased. From figure 12, it can be observed that an increase in the maximum efficiency of forest management programs to increase the forest biomass (η_1) dampens the periodic oscillations and after a critical value of η_1 the periodic oscillation dies out and the solution trajectories of the system (5) settle to a positive equilibrium state. This shows that the implementation of forest management

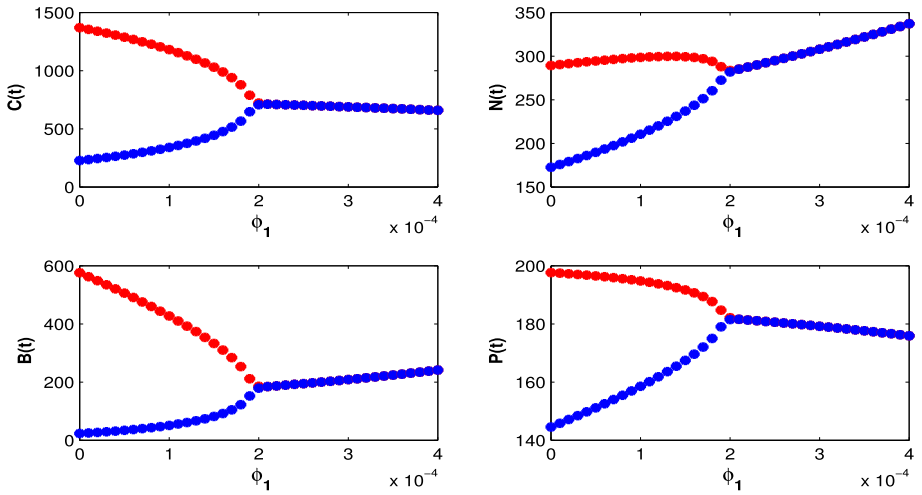

Fig. 11 Bifurcation diagrams of atmospheric carbon dioxide, human population, forest biomass and forest management programs with respect to ϕ_1 at $\phi = 0.0008$. The other parameters take same values as in Table 1

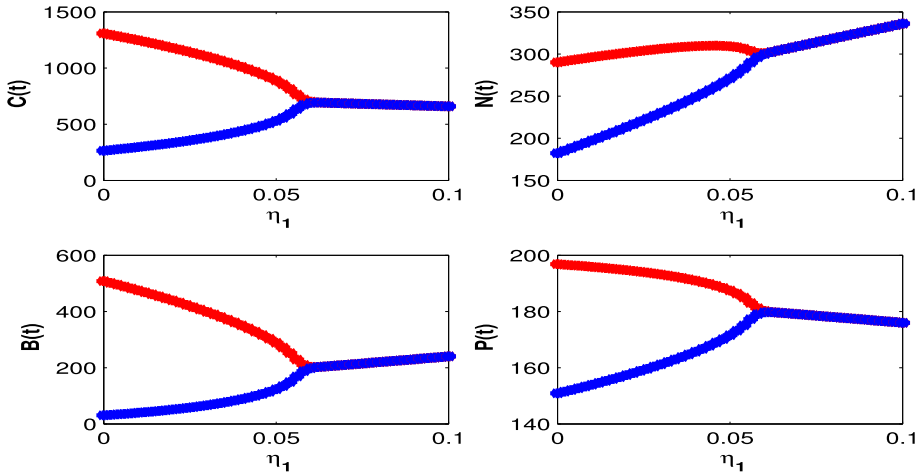

Fig. 12 Bifurcation diagrams of atmospheric carbon dioxide, human population, forest biomass and forest management programs with respect to η_1 at $\phi = 0.0008$. The other parameters take same values as in Table 1

programs not only decreases the atmospheric CO_2 level but can enhance the stability of the positive equilibrium state of the system.

The optimality system is solved numerically by taking weight factors $w_1 = 1$ and $w_2 = 15000$, $v_{\max} = 0.02$, and $t_f = 100$. The atmospheric CO_2 concentration and forest biomass in the absence and presence of optimal control, and the profile of the time -dependent control $v(t)$ is shown in figure 13. This figure shows an increase in forest biomass and a drop in atmospheric CO_2 concentration in the presence of time-dependent control $v(t)$. The optimal profile of $v(t)$ shows that it is optimal to execute the forest management programs at the maximum level for first 67 months and reduce gradually afterward. The optimal profile of the control parameter for different values of $v_{\max}$ is depicted in the first plot of figure

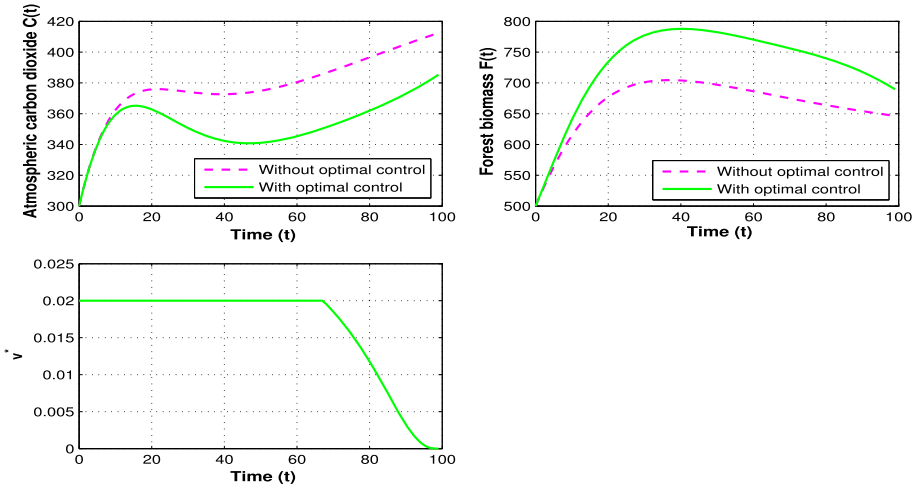

Fig. 13 Future concentration of CO_2 and forest biomass with and without optimal control and optimal profile of control parameter $v(t)$. The other parameter values are same as in Table 1 with $t_f = 100$, $v_{\max} = 0.02$, $w_1 = 1$ and $w_2 = 15000$

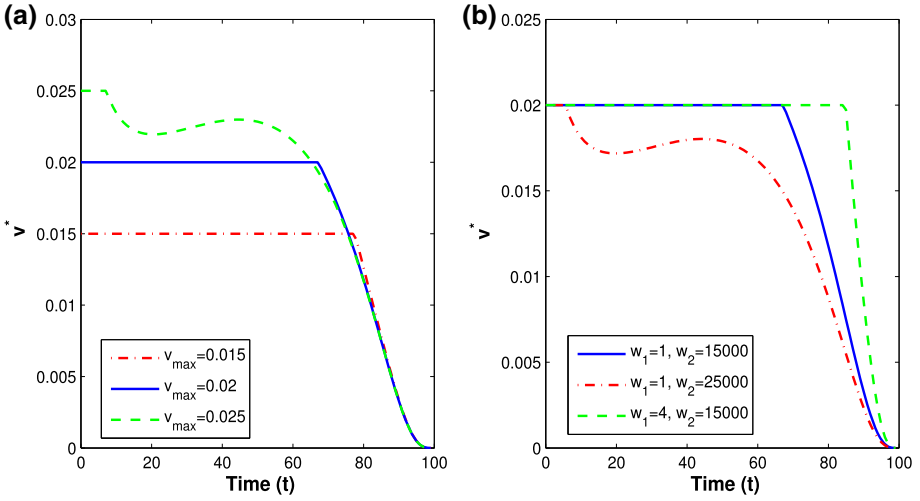

Fig. 14 The optimal profile of $v(t)$ for different values of **a** $v_{\max}$ at $w_1 = 1$ and $w_2 = 15000$, and **b** for different values of w_1 and w_2 at $v_{\max} = 0.02$. The other parameters take same value as in Table 1 with $t_f = 100$

14, showing that time span over which the forest management programs are executed at maximum level reduces with an increase in the value of $v_{\max}$. The second plot of figure 14 shows that the time span over which the management programs are implemented at a maximum rate also reduces with an increase in w_2 while it increases with an increase in w_1. Thus if the weight of the cost of implementation of management programs is high, the programs are applied at the maximum rate for a lesser period and reduced afterward. The effect of varying some parameters namely, ϕ_1, η_1, l_1, k_1, and $v_{\max}$ on the cost functional J is illustrated in figure 15. This indicates that the cost functional increases with the increase

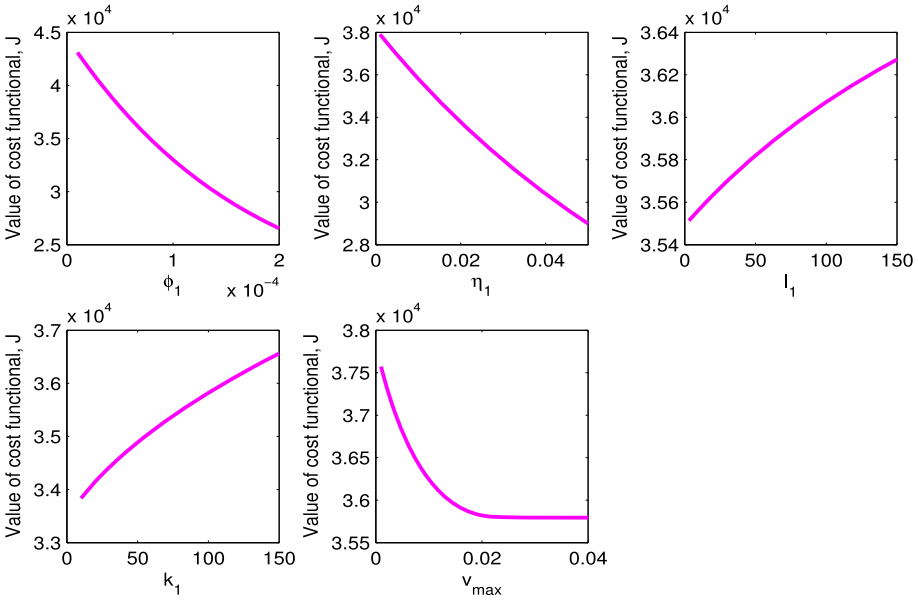

Fig. 15 Effect of varying ϕ_1, η_1, l_1, k_1 and $\upsilon_{\max}$ on cost functional J and the other parameter values are same as in Table 1 with $t_f = 100,\ \upsilon_{\max} = 0.02,\ w_1 = 1$ and $w_2 = 15000$

in the half-saturation constants k_1 and l_1 and decreases with the increase in the maximum efficacy of forest management programs to reduce the deforestation rate ϕ_1, the maximum efficacy of forest management programs to increase the forest biomass η_1 and the maximum implementation rate of control $\upsilon_{\max}$.

6 Conclusion

The sustainable management of forests can play a key role in climate change mitigation by reducing the atmospheric burden of the prime greenhouse gas, carbon dioxide. In the present work, a mathematical model is presented to analyze the effect of forest management programs over the control of CO_2 levels in the Earth's atmosphere. The model under consideration is governed by four nonlinear differential equations capturing the dynamic relationship between CO_2 concentration, human population, forest biomass and forest management programs. It is considered that the forest management programs focus on increasing the forest biomass and reducing the deforestation rate. The reduction in the deforestation rate and increase in the growth rate of forest biomass due to forest management programs are taken to be a nonlinear saturating function of forest management programs. A comprehensive stability analysis of the equilibrium states of the proposed model is performed and the conditions for the local and global stability of the equilibria are derived. The model analysis shows that the equilibrium levels of CO_2 can be reduced by increasing the implementation rate and maximum efficiencies of forest management programs to reduce the deforestation rate and increase the forest biomass, respectively. It is shown that the use of forest management policies in which the reduction in the deforestation rate and increase in the growth rate of forest biomass increase more rapidly at low implementation cost are more beneficial in increasing

the forest cover and reducing the atmospheric burden of CO_2 gas. Model analysis shows that a sudden change in the dynamics of the system about the positive equilibrium S^* may occur as the deforestation rate varies. It is found that the loss of stability of positive equilibrium S^* occurs as the deforestation rate ϕ crosses a critical threshold ϕ_c with generation of sustained oscillations about S^* via Hopf-bifurcation. The conditions for existence of Hopf-bifurcation with respect to parameter ϕ are derived. It is shown that if the deforestation rate $\phi < \phi_c$, the positive equilibrium S^* is stable, and the atmospheric CO_2 and other model variables attain positive equilibrium levels. However, for $\phi > \phi_c$, all the model variables show oscillator characteristics. The stability and direction of periodic solutions are also analyzed using the center manifold theory.

It is observed that an increase in the maximum efficiencies of the forest management programs to reduce the deforestation rate (ϕ_1) and increase the forest biomass (η_1), respectively, can dampen the oscillations in the atmospheric CO_2 level that have been arisen due to increase in the deforestation rate above the threshold value ϕ_c. These periodic oscillations may even die out and positive equilibrium S^* again becomes stable as ϕ_1 or η_1 crosses the critical value. This shows that an increase in maximum efficiencies of forest management programs to slow down the deforestation rate and increase the forest biomass not only reduce the equilibrium level of CO_2 but exert a stabilizing effect on the system's dynamics. Although the forest management programs have the potential to reduce the atmospheric burden to CO_2, but their execution cost is one of the prime barriers to their execution on a large scale. Using optimal control theory, we have derived the management policies that reduce the CO_2 emission at minimum implementation cost. For this purpose, we have taken the increased execution rate of forest management programs as time dependent function $v(t)$ on some finite time interval and derived the optimal profile of $v(t)$ that minimizes the cost functional. It is found that the cost functional decreases with an increase in the maximum efficacy of forest management programs to reduce the deforestation rate (ϕ_1), the maximum efficacy of forest management programs to increase the forest biomass (η_1) and the maximum implementation rate of control ($v_{\max}$). This suggests that the cost effective forest management policies must include those technological options that have high efficiency to increase the forest biomass such as plantation of genetically engineered trees. Apart from this, forest management policies must include programs that cause reduction in deforestation rate, such as education programs that motivate the people to reduce the use of wood based products, providing economic incentives to rural population to switch to fuel efficient stoves and biogas, etc. Overall, the present study provides a mathematical framework to assess the effect of forest management policies over the reduction of CO_2 level while minimizing the implementation cost.

Declarations

Conflict of interest The authors declare that they have no conflict of interest with regard to this article.

References

Badola R, Barthwal S, Hussain SA (2012) Attitudes of local communities towards conservation of mangrove forests: a case study from the east coast of India. Estuar Coast Shelf Sci 96:188–196

Basu JP (2014) Agroforestry, climate change mitigation and livelihood security in India. N Z J For Sci 44(Suppl 1):S11

Bottazzi P, Cattaneo A, Rocha DC, Rist S (2013) Assessing sustainable forest management under REDD+: a community-based labour perspective. Ecol Econ 93:94–103

Caetano MAL, Gherardi DFM, Yoneyama T (2011) An optimized policy for the reduction of CO_2 emission in the Brazilian Legal Amazon. Ecol Model 222:2835–2840
Casper JK (2010) Greenhouse gases: Worldwide impacts. Facts On File Inc, New York
Chang S, Mahon EL, MacKay HA, Rottmann WH, Strauss SH, Pijut PM, Powell WA, Coffey V, Lu H, Mansfield SD, Jones TJ (2018) Genetic engineering of trees: progress and new horizons. In Vitro Cell Dev Biol Plant 54:341–376
Devi S, Gupta N (2018) Dynamics of carbon dioxide gas (CO_2): effects of varying capability of plants to absorb CO_2. Nat Resour Model 32:e12174
Devi S, Gupta N (2020) Comparative study of the effects of different growths of vegetation biomass on CO_2 in crisp and fuzzy environments. Nat Resour Model 33:e12263
Devi S, Mishra RP (2020) Preservation of the forestry biomass and control of increasing atmospheric CO_2 using concept of reserved forestry biomass. Int J Appl Comput Math 6:17
Dubey B, Sharma S, Sinha P, Shukla JB (2009) Modelling the depletion of forestry resources by population and population pressure augmented industrialization. Appl Math Model 33:3002–3014
Dubouzet JG, Strabala TJ, Wagner A (2013) Potential transgenic routes to increase tree biomass. Plant Sci 212:72–101
FAO (2016) Global forest resources assessment 2015: How are the world's forests changing?, 2nd edn. Food and Agriculture Organization of the United Nations, Rome, p 54
FAO (2020) Global forest resources assessment 2020-Key findings. Rome. https://doi.org/10.4060/ca8753en
Fleming WH, Rishel RW (1975) Deterministic and stochastic optimal control. Springer, New York
Harfouche A, Meilan R, Altman A (2011) Tree genetic engineering and applications to sustainable forestry and biomass production. Trends Biotechnol 29(1):9–17
Hassard BD, Kazarinoff ND, Wan YH (1981) Theory and application of Hopf-bifurcation. Cambridge University Press, Cambridge, pp 181–219
Ichikawa A (2004) Impacts and risks of global warming. In: Ichikawa A (ed) Global warming-the research challenges. Springer, Berlin, pp 85-114
IPCC (2014) Climate Change 2014: Synthesis report. In: Contribution of Working Groups I, II and III to the fifth Assessment Report of the Intergovernmental Panel on Climate Change [Core Writing Team, Pachauri RK, Meyer LA (eds)]. IPCC, Geneva, Switzerland, 151 pp
Jackson RB, Baker JS (2010) Opportunities and constraints for forest climate mitigation. BioScience 60:698–707
Jorgenson AK, Clark B (2013) The relationship between national-level carbon dioxide emissions and population size: an assessment of regional and temporal variation, 1960–2005. PLoS One 8(2):e57107
Kurane I (2010) The effect of global warming on infectious diseases. Osong Public Health Res Perspect 1(1):4–9
Lata K, Misra AK (2017) Modeling the effect of economic efforts to control population pressure and conserve forestry resources. Nonlinear Anal Model Control 22(4):473–488
Ledford H (2014) Brazil considers transgenic trees: genetically modified eucalyptus could be a global test case. Nature 512:357
Lonngren KE, Bai EW (2008) On the global warming problem due to carbon dioxide. Energy Policy 36:1567–1568
Lukes DL (1982) Differential equations: classical to controlled. In: Mathematics in science and engineering, vol 162. Academic Press, New York
McMichael AJ, Woodruff RE, Hales S (2006) Climate change and human health: present and future risks. Lancet 367:859–869
Misra AK (2014) Climate change and challenges of water and food security. Int J Sustain Built Environ 3(1):153–165
Misra AK, Jha A (2021) Modeling the effect of population pressure on the dynamics of carbon dioxide gas. J Appl Math Comput 67(2):623–640
Misra AK, Lata K (2015a) A mathematical model to achieve sustainable forest management. Int J Model Simul Sci Comput 6(4):1550040
Misra AK, Lata K (2015b) Depletion and conservation of forestry resources: a mathematical Model. Differ Equ Dyn Syst 23(1):25–41
Misra AK, Verma M (2013) A mathematical model to study the dynamics of carbon dioxide gas in the atmosphere. Appl Math Comput 219:8595–8609
Misra AK, Verma M (2015) Impact of environmental education on mitigation of carbon dioxide emissions: a modelling study. Int J Glob Warm 7:466–486
Misra AK, Verma M, Venturino E (2015) Modeling the control of atmospheric carbon dioxide through reforestation: effect of time delay. Model Earth Syst Environ 1:24

Nikol'kii MS (2010) A controlled model of carbon circulation between the atmosphere and the ocean. Comput Math Model 21:414–424
NOAA (2022) Trends in atmospheric carbon dioxide. https://gml.noaa.gov/ccgg/trends/
Onozaki K (2009) Population is a critical factor for global carbon dioxide increase. J Health Sci 55:125–127
Prentice IC, Farquhar GD, Fasham MJR, Goulden ML, Heimann M, Jaramillo VJ, Kheshgi HS, Le Quere C, Scholes RJ, Wallace DWR (2001) The Carbon Cycle and Atmospheric Carbon Dioxide. In: Climate Change: the Scientific Basis. Contributions of Working Group I to the Third Assessment Report of the Intergovernmental Panel on Climate Change. Houghton JT, Ding Y, Griggs DJ, Noguer M, Linden PJVD, Dai X, Maskell K, Johnson CA (eds). Cambridge University Press, Cambridge, UK, pp 185-237
Roopsind A, Sohngen B, Brandt J (2019) Evidence that a national REDD+ program reduces tree cover loss and carbon emissions in a high forest cover, low deforestation country. Proc Natl Acad Sci USA 116:24492–24499
Shukla JB, Dubey B (1997) Modelling the depletion and conservation of forestry resources: effects of population and pollution. J Math Biol 36:71–94
Shukla JB, Chauhan MS, Sundar S, Naresh R (2015) Removal of carbon dioxide from the atmosphere to reduce global warming: a modeling study. Int J Glob Warm 7(2):270–292
Shuman EK (2010) Global climate change and infectious diseases. N Engl J Med 362:1061–1063
Tafoya KA, Brondizio ES, Johnson CE, Beck P, Wallace M, Quiros R, Wasserman MD (2020) Effectiveness of Costa Rica's conservation portfolio to lower deforestation, protect primates, and increase community participation. Front Environ Sci 8:580724
Tennakone K (1990) Stability of the biomass-carbon dioxide equilibrium in the atmosphere: mathematical model. Appl Math Comput 35:125–130
UNFCCC (2010) Report of the Conference of the Parties on its fifteenth session, held in Copenhagen from 7 to 19 December 2009. Framework Convention on Climate. https://unfccc.int/resource/docs/2009/cop15/eng/11a01.pdf Change
Van Noordwijk M, Roshetko JM, Murniati, Angeles MD, Suyanto, Fay C and Tomich TP (2003) Agroforestry is a Form of Sustainable Forest Management: Lessons from South East Asia. ICRAF Southeast Asia Working Paper No. 2003-2. World Agroforestry Centre -ICRAF, SEA Regional Office, Bogor, Indonesia, p 18
Verma M, Misra AK (2018) Optimal control of anthropogenic carbon dioxide emissions through technological options: a modeling study. Comput Appl Math 37:605–626
Verma M, Verma AK (2021) Effect of plantation of genetically modified trees on the control of atmospheric carbon dioxide: a modeling study. Nat Resour Model 34(2):e12300
Verma M, Verma AK, Misra AK (2021) Mathematical modeling and optimal control of carbon dioxide emissions from energy sector. Environ Dev Sustain 23:13919–13944
Yang J, Zhou M, Ren Z, Li M, Wang B, Liu DL, Ou CQ, Yin P, Sun J, Tong S, Wang H, Zhang C, Wang J, Guo Y, Liu Q (2021) Projecting heat-related excess mortality under climate change scenarios in China. Nat Commun 12:1039
Ye X, Busov V, Zhao N, Meilan R, McDonnell LM, Coleman HD, Mansfield SD, Chen F, Li Y, Cheng ZM (2011) Transgenic populus trees for forest products, bioenergy, and functional genomics. Crit Rev Plant Sci 30:415–434
Zomer RJ, Neufeldt H, Xu J, Ahrends A, Bossio D, Trabucco A, Van Noordwijk M, Wang M (2016) Global tree cover and biomass carbon on agricultural land: the contribution of agroforestry to global and national carbon budgets. Sci Rep 6:29987